



## THE STUDY OF THE ANTIOXIDATIVE AND CATALYTIC ACTIVITIES OF NI NANOPARTICLES SYNTHESIZED FROM *TERMINALIA CHEBULA* EXTRACT

Md. Moulana Kareem<sup>1</sup>, Hari Babu<sup>2</sup>, G. Vijaya Lakshmi\*<sup>3</sup>

<sup>1</sup>Department of Chemistry, Government Degree College, Manugur, Telangana, India

<sup>2</sup>Department of Chemistry, MALD Government Degree College, Gadwal, Telangana, India

<sup>3</sup>Department of Chemistry, University College for Women, Koti, Osmania University, Hyderabad, Telangana, India

\*Corresponding author: [gvjlakshmi@gmail.com](mailto:gvjlakshmi@gmail.com)

Received: 16-03-2022; Revised & Accepted: 06-07-2022; Published: 31-07-2022

© Creative Commons Attribution-NonCommercial-NoDerivatives 4.0 International License <https://doi.org/10.55218/JASR.202213604>

### ABSTRACT

The catalytic activity of Ni NPs can be utilized to alleviate environment pollution caused by industrial effluents containing organic dyes. In the present work, a green method was employed for the synthesis of Nickel (Ni) nanoparticles using Polyphenolic rich *Terminalia Chebula* fruit aqueous extract and evaluated its catalytic activity against carcinogenic congo red dye along with antioxidant activity. The UV-Vis peak at 395 nm revealed the formation and monodispersed nature of nanoparticle. FTIR studies confirmed that polyphenolic and alkaloids were utilized in the formation of nanoparticles. The XRD established formation of Ni nanoparticles of FCC. SEM indicated the agglomeration of nanoparticles and TEM established the spherical shape with an average size about 6-8 nm. This study also evaluated the catalytic and antioxidant activities of green synthesized Ni NPs. Catalytic degradation of carcinogenic congo red dye completed within 20 mints, degradation of the congo red dye found to be first order kinetics, antioxidant activity against DPPH found maximum to 100 µg/ml and EC<sub>50</sub> as 65.01.

**Keywords:** Antioxidant, Catalytic, Eco-friendly, Nickel nanoparticles, Polyphenols.

### 1. INTRODUCTION

Industries have been dumping untreated water straight into the environment, poisoning land and water bodies with dangerous metals, dyes, pesticides, and insecticides, in violation of environmental authority rule [1, 2]. The dyeing industry is responsible for 17-20% of all industrial water pollution. Congo red (CR) is an azo dye that is the sodium salt of 3, 3'-([1,1'-biphenyl]-4,4'-diyl) bis ([1,1'-biphenyl]-4,4'-diyl) bis ([1,1'-biphenyl]-4,4'-diyl) bis ([1,1 (4-amino naphthalene-1-sulfonic acid) [3].

Because color impacts light quality and reduces underwater light penetration, resulting in lower dissolved O<sub>2</sub> concentrations, azo dye-containing wastewater has a significant impact on photosynthetic activity in aquatic environments [4]. In humans, CR can cause anorexia, weakness, gastrointestinal distress and other health problems. The CR dye is a secondary organic di-azo dye with complex aromatic components that make the dye more persistent and non-degradable, making removal difficult [5, 6]. Several physical,

biological and chemical processes are available to remove colorants from industrial effluents, including electrochemical treatment, aerobic and anaerobic microbial degradation, and photochemical degradation and ion exchange [7-10].

Nanoparticles such as Ni, Ag, Au, ZnO, CuO, CdO, NiO and others are effective in green-remediation and organic dye treatment of polluted water [11,12]. Some degradation products, such as benzidine, may be more dangerous than the colorant itself, and due to their high cost, these techniques are rarely used. Catalytic hydrogenation easily breaks the azo bonds of azo dye molecules. This means that the dye molecules can be converted into less toxic, more environmentally friendly chemicals [13, 14].

Because of their unique magnetic, catalytic and electrical properties, nickel (Ni) nanoparticles (NPs) are extremely important in energy technology, magnetism, green medicine, and electronics. These NPs, which have high chemical stability, super capacitance, electron transfer capacity, and electro catalysis, are used in green

therapeutics as well as photo catalytic, anti-inflammatory and antibacterial activities [15].

Nanoparticles can be prepared using a variety of chemical and physical methods, most of which are costly and hazardous to the environment. The increase in global pollution has compelled scientists to develop a new, environment friendly, and cost-effective method for preparing nanoparticles [16]. Green synthesis is a bottom-up strategy, similar to chemical reduction. In this procedure, expensive chemicals such as reducing and stabilizing agents are replaced with extracts from a biological system. Plants are regarded as the most promising biological resources for the synthesis of nanoparticles due to their faster reduction rate, simplicity and ease of supply [17].

*Terminalia chebula* (*T. chebula*) is a *Combretaceae* family evergreen blooming tree. Tannins, flavonoids, sterols, amino acids, fructose, resin, fixed oils, and other phytoconstituents are found in *T. chebula*. Chebulic acid, chebulinic acid, chebulagic acid, gallic acid, corilagin and ellagic acids are the principal components of hydrolysable tannins, which allow the production of Ni NPs and oxidised polyphenols may function as stabilizing agents [18, 19]. This study is the first to describe *T. chebula* aqueous extract-mediated green production of Ni NPs using Nickel nitrate solution.

The goal of this study is to synthesize Ni NPs using *T. chebula* fruit extract as a reducing and stabilizing agent in a simple, inexpensive and eco friendly manner. We examined the catalytic and antioxidant properties of biogenic Ni NPs against Congo red dye in aqueous solution and the DPPH free radical.

## 2. MATERIAL AND METHODS

*Terminalia chebula* fruit purchased from local market and analytical grade of all the reagents procured were used without purification for the synthesis of Ni nanoparticles, such as Nickel Nitrite ( $\text{Ni}(\text{NO}_3)_2$ ), sodium hydroxide (NaOH), Congo Red dye (CR), DPPH (2,2-diphenyl-1-picrylhydrazyl), Methanol, Ascorbic acid and sodium borohydride ( $\text{NaBH}_4$ ).

### 2.1. Preparation of Aqueous Extracts

One gm of finely powdered *T. chebula* was transferred to a clean 250ml conical flask containing 100ml of distilled water and stirred for 40 minutes at 60°C. Then after the extract was cooled to room temperature and filtered with Whatmann filter paper no.1, filtrate were collected and centrifuged at 4000 rpm for 15 mins. Finally, the recovered fruit extract filtrate was stored at 4°C [19].

### 2.2. Biosynthesis of Ni nanoparticles (Ni NPs)

To perform green-synthesis of Ni NPs, 20 ml of *T. chebula* fruit aqueous extract was mixed with 90 ml of 3 mM  $\text{NiCl}_2$  solution, followed by a dropwise addition of 10 ml of NaOH solution (0.1 M) to keep the reaction mixture pH at 12. The reaction mixture was then heated on a magnetic stirrer at 80°C for 75 minutes, and the production of Ni NPs was identified by a color changes from pale yellow to brown [20]. The reaction mixture was then centrifuged for 20 minutes at 4000 rpm, the supernatant was discarded, and the residue containing Ni NPs was re-dispersed twice in distilled water to remove phytochemicals that had adhered to the surface of the Ni NPs. The Ni NPs residue was dried in an oven at 80°C for 2 hours before being pulverised and stored for future experiments.

### 2.3. Characterization

The UV-Vis spectra of green-synthesised nanoparticles were obtained in the wavelength range of 200-800 nm with a resolution of 1 nm using a UV-Visible spectrophotometer (Lab India UV-3000+). Fourier transform infrared (FTIR) absorption spectra of dried nanoparticles were acquired with an FT-IR spectrophotometer (Shimadzu) utilising KBr pellets and scanned in the 400-4000 $\text{cm}^{-1}$  range. The structural characteristics were examined using an XRD using a Bruker D-8 Advance X-ray Diffractometer with a monochromatic CuK source. A scanning electron microscopy (SEM) picture and energy dispersive spectra (EDS) were obtained using a JEOL JSM6360 SEM. Transmission electron microscopy (TEM) measurements and selected-area electron diffraction (SAED) patterns were performed using a TEM (JEOL JEM-2100F) at a 200 kV accelerating voltage.

### 2.4. Determination of antioxidant activity DPPH (2'2-Diphenyl-1-picrylhydrazyl) assay

The free radical scavenging activity of green-synthesized Ni NPs was determined using the DPPH assay, which was modified slightly from the procedure described by Khan et al [21]. The reaction mixture dilution series was prepared by incubating different concentrations of green-synthesized Ni NPs (10-100 g/ml) in 3ml of 4 percent DPPH solutions in methanol for 30 minutes at room temperature. When the green-synthesized Ni NPs were oxidised, the DPPH, a stable purple-colored free radical (DPPH), changed into a colourless molecule (-diphenyl -picryl hydrazine). The extent of discolouration shows the quantity of DPPH scavenged

by green-synthesized Ni NPs. The absorbance of the control (no Ni NPs) and test samples was measured at 517nm. Ascorbic acid is a well-known antioxidant. The % inhibition of DPPH calculated by the following formula:

$$\text{The \% inhibition of DPPH} = [(C-T)/C] \times 100$$

Where C is the absorbance of control and T is the absorbance of the test sample.

## 2.5. Photo Catalytic degradation of Congo Red dye

Catalytic degradation of Congo red (CR) was carried out with green synthesized Ni NPs in presence of sodium borohydride. About 100 mL of 0.05M Congo red dye solution was added to 2 ml of 0.5M sodium borohydride solution containing conical flask at room temperature and mixed well with a stirrer for 5 mints. The reaction mixture was then subjected to exposure of sun light with the addition of 5 mg of TC-Ni NPs. The dark red color of the reaction mixture started fading indicated the catalytic degradation of dye. The absorbance of this reaction medium was monitored using UV-Vis spectrophotometer (LAB INDIA UV-3000) at 492 nm at regular time intervals of 5 mints [20]. Congo red degradation percentage was calculated using the following equation:

$$\text{CR degradation (\%)} = [(A_o - A_t)/A_o] \times 100$$

Where  $A_o$  is the initial absorbance of CR solution without Ni NPs (control) and  $A_t$  is absorbance of the CR solution after t mints.

## 3. RESULTS AND DISCUSSION

### 3.1. UV-VIS spectroscopy

Fig. 1 depicts the UV maximum absorption peak of nickel nanoparticles formed at 395 nm, which is prominent and sharp. The peak's intensity and sharpness show that the generated NPs were well dispersed, stable and high yielding. Ni nanoparticles have a characteristic absorbance peak that ranges from 230nm to 400nm [23]. The original yellow color of the solution changed to a brown precipitate because of surface Plasmon resonance.

### 3.2. FTIR Spectroscopy

The FTIR spectra shown in fig. 2 give information regarding the functional groups present in *T. chebula* aqueous extract as well as those responsible for the synthesis of Ni NPs. The bands at  $2786 \text{ cm}^{-1}$  and  $3480 \text{ cm}^{-1}$  correspond to -C-N and -OH stretching,

respectively. The band at  $1740 \text{ cm}^{-1}$  is caused by -C O stretching. The IR bands seen at  $1400$  and  $1035 \text{ cm}^{-1}$  can be attributed to the -C-O and -C-O-C stretching modes, respectively.

The FTIR of NPs showed a decrease in the intensity and broadness of O-H and C=O stretching signals, indicating the consumption of flavonoid and polyphenolic extract metabolites in the biogenic synthesis of Ni NPs [27]. The increased stability of NPs due to phytochemical capping in *T. chebula* aqueous extracts FT-IR analysis clearly demonstrates this. *T. chebula* aqueous extract contains a high concentration of hydrolyzed tannins in form of polyphenolic compounds, and which aids in the reduction of  $\text{Ni}^{2+}$  to Ni NPs [28].

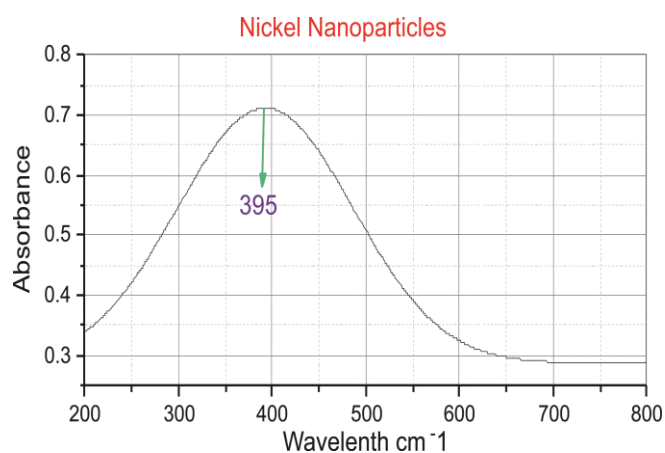


Fig. 1: UV-Visible spectra

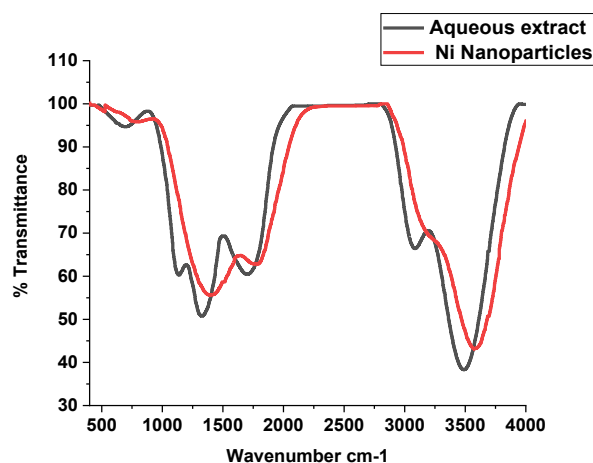


Fig. 2: FTIR spectra of *T. Chebula* fruit extract and Ni NPs

### 3.3. XRD (Crystallographic) analysis

The X-ray diffraction pattern of bio-synthesized Ni nanoparticles is shown in fig. 3. From the XRD patterns, Ni exhibits sharp peak reflections at position

$2\theta = 43.11^\circ$ ,  $50.25^\circ$ , and  $74.113^\circ$  corresponds to (111) (200) (220) reflection of Ni face centred cubic (fcc) structure with space group Fm-3m for cubic lattice constant  $3.5214 \text{ \AA}$  respectively, and apart from these three peaks, low-intensity peaks observed around at

$36.54^\circ$ ,  $39.12^\circ$  indicates the formation of a trace amount of Nickel oxide. The results were well matched with Nickel JCPDS standard powder diffraction card, file No. JCPDS No. 04-0835[29].



**Fig. 3: XRD patterns of bio-synthesized Ni NPs sample**

### 3.4. Morphological Investigations

SEM study evidenced the production of Ni NPs as well as their morphological dimensions. Fig. 4 depicts the presence of 40-60 nm average size Ni NPs that are distributed and uneven in shape, with the presence of voids [15]. Large particles up to  $4\text{-}5\mu\text{m}$  in size were discovered. This could be attributed to NP agglomeration and magnetic interaction between the NPs [21].

TEM of *T. chebula* mediated Ni NPs is shown in Fig. 5a-d. It is observed from figure that the Ni NPs have an average size of 7-8 nm (Fig-5e) and are spherical in shape (Fig.5a-d). The associated selected area electron diffraction (SAED) patterns represent the polycrystalline nature that has been demonstrated (Fig-5f). The initial rings contributed for Ni at (111) reflection at d-spacing  $0.40858$  for cubic structure, according to SAED patterns indexing. The SAED pattern results are consistent with the XRD results.

### 3.5. Scavenging activity of Ni nanoparticles

The antioxidant activity of *T. Chebula*-Ni NPs was investigated using the DPPH free radical scavenging test. *T. Chebula*-Ni NPs has shown remarkable DPPH

radical scavenging activity in a dose-dependent manner (Figs. 6a-b & Table 1). The results revealed that the antioxidant activity was directly proportional to the concentration of *T. Chebula*-Ni NPs. The  $EC_{50}$  (effective concentration required to inhibit 50% of free radicals) of *T. Chebula*-Ni NPs was found to be 65.01 and, the  $EC_{50}$  value of ascorbic acid (reference standard) was 52.78 for DPPH radical scavenging activities, respectively. Lower the  $EC_{50}$  values, more ease to hydrogen donating capacity and thus more the antioxidant activity of the free radical scavengers. Among the various concentrations of Ni NPs examined,  $100 \mu\text{g/ml}$  had the highest scavenging activity (78.51 percent) and  $20 \mu\text{g/ml}$  had the lowest (11.56 percent). Table 1 shows the dose-dependent antioxidant activity of Ni NPs. The extraordinary antioxidant potential of Ni nanoparticles can be attributed to the electron-donating character of the negatively charged nanoparticles surface, which may be responsible for free radical species or hydroxyl ion scavenging [31]. As a result, this study found that green-synthesized Ni NPs exhibited equivalent antioxidant activity to ascorbic acid against DPPH [32].

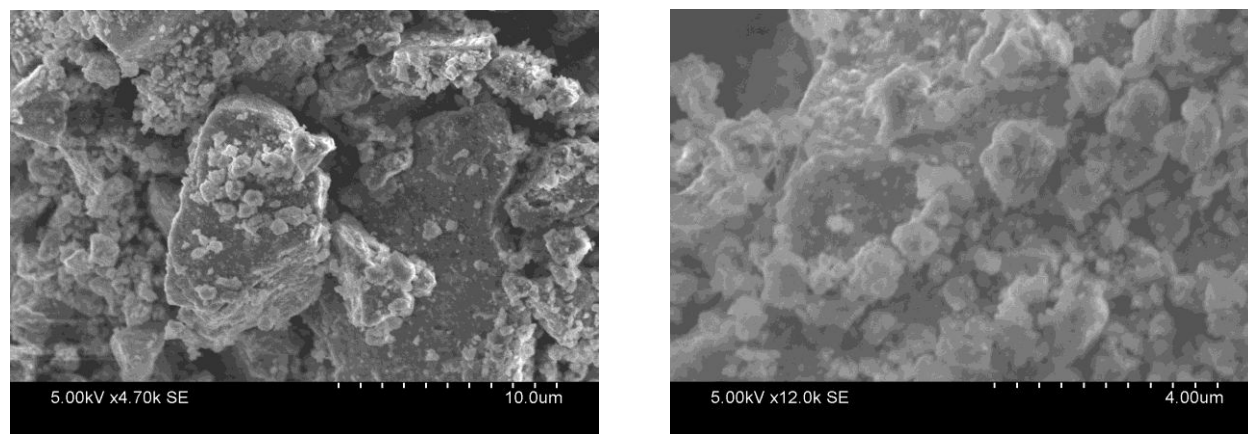


Fig. 4: SEM images of Ni NPs

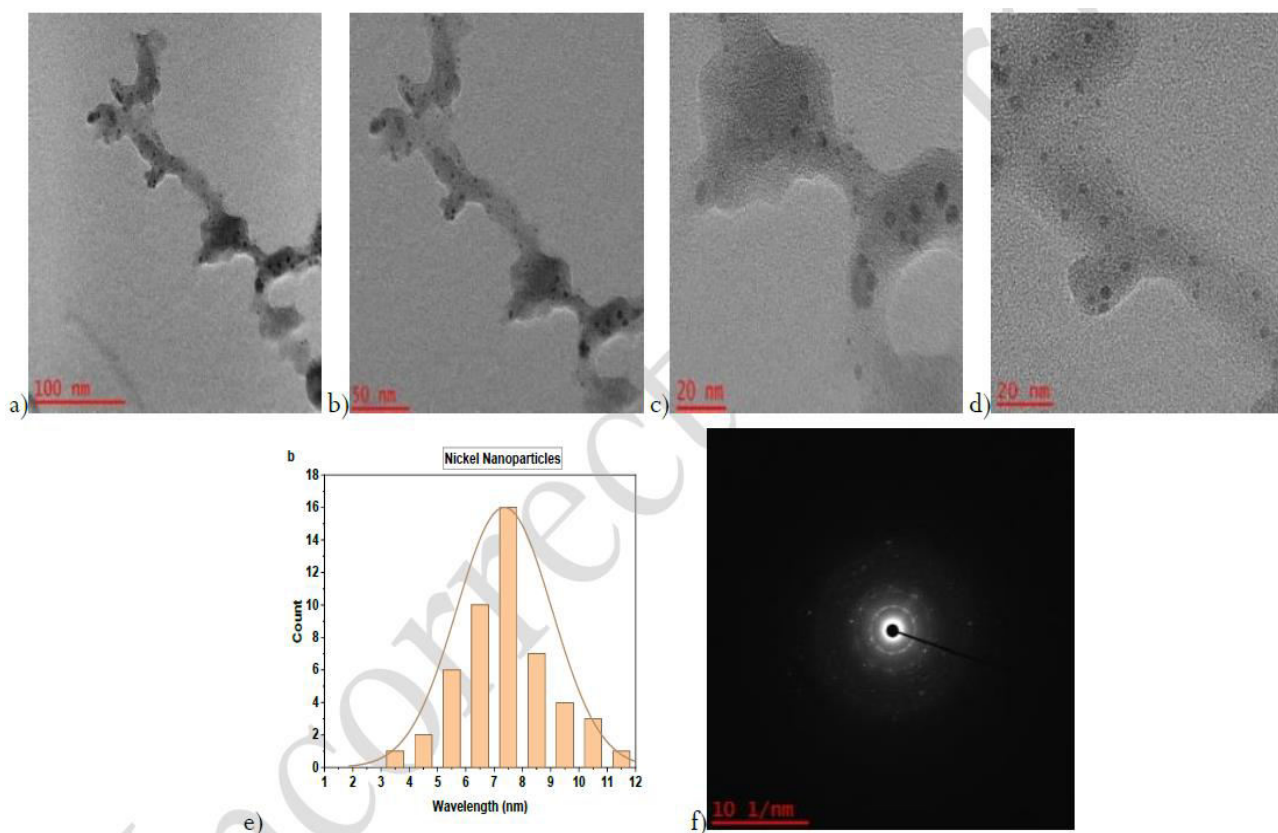


Fig. 5a-d: TEM image of Ni NPs, e) Histogram of Ni NPs, f) SAED of Ni NPs

Table 1: Dose dependent Scavenging activity of ascorbic acid and green-synthesized Ni NPs

S. No	Volume of DPPH	Concentration of Ascorbic acid	Concentration of Ni NPs	% of Scavenging Activity of Ascorbic acid	% of Scavenging Activity of Ni NPs	EC50 of Ni NPs	EC 50 of Ascorbic acid
1	3 ml	20 $\mu\text{g/ml}$	20 $\mu\text{g/ml}$	16.34	11.56		
2	3 ml	40 $\mu\text{g/ml}$	40 $\mu\text{g/ml}$	44.23	32.58		
3	3 ml	60 $\mu\text{g/ml}$	60 $\mu\text{g/ml}$	55.76	44.12	65.01	52.78
4	3 ml	80 $\mu\text{g/ml}$	80 $\mu\text{g/ml}$	76.92	62.68		
5	3 ml	100 $\mu\text{g/ml}$	100 $\mu\text{g/ml}$	90.38	78.51		

### 3.6. Photo Catalytic degradation of Congo red Dye

The reduction of CR was carried out in the presence of *T. Chebula*-Ni NPs and NaBH<sub>4</sub> using a UV-visible spectrometer within the wavelength range of 400-800 nm. The UV-visible spectrum of CR (blank) gives strong absorption peaks at 492 nm. In the absence of a catalyst, the peak intensity remains unaffected. However, with the addition of 5 mg of Ni NPs, the decrease in peak intensity at 492 nm started. The reduction of CR was monitored using a UV-visible spectrometer at a regular time interval of 5 min between successive measurements, as shown in Fig. 7a. With the addition of *T. Chebula*-Ni NPs, the intensity of

the peak decreases due to the reduction of CR dye. Thus, the gradual decrease in intensity of peaks at 492 nm was measured using a UV-visible spectrometer. The photocatalytic degradation of Congo red dye was completed in 20 mints during the reduction process. The percent reduction of CR dye as a function of time is depicted in Fig. 7b.

Despite the fact that NaBH<sub>4</sub> can not reduce CR in the absence of a catalyst, the reduction of CR follows first-order kinetics [33]. The linear plot of  $\ln(C_0/C_t)$  vs. reduction time revealed the rate constant of the (reduction of CR) pseudo-first-order reaction as  $1.46 \times 10^{-2} \pm 0.0078 \text{ sec}^{-1}$ .

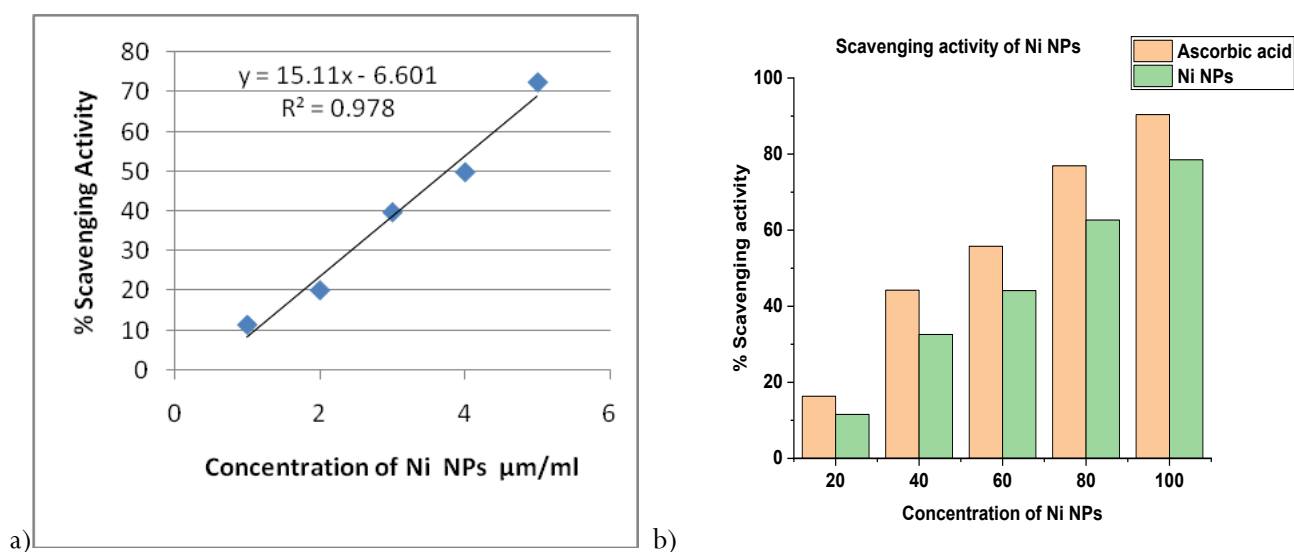


Fig. 6: a) Plot of scavenging activity of Ni NPs, b) Scavenging activity of Ni NPs and ascorbic acid

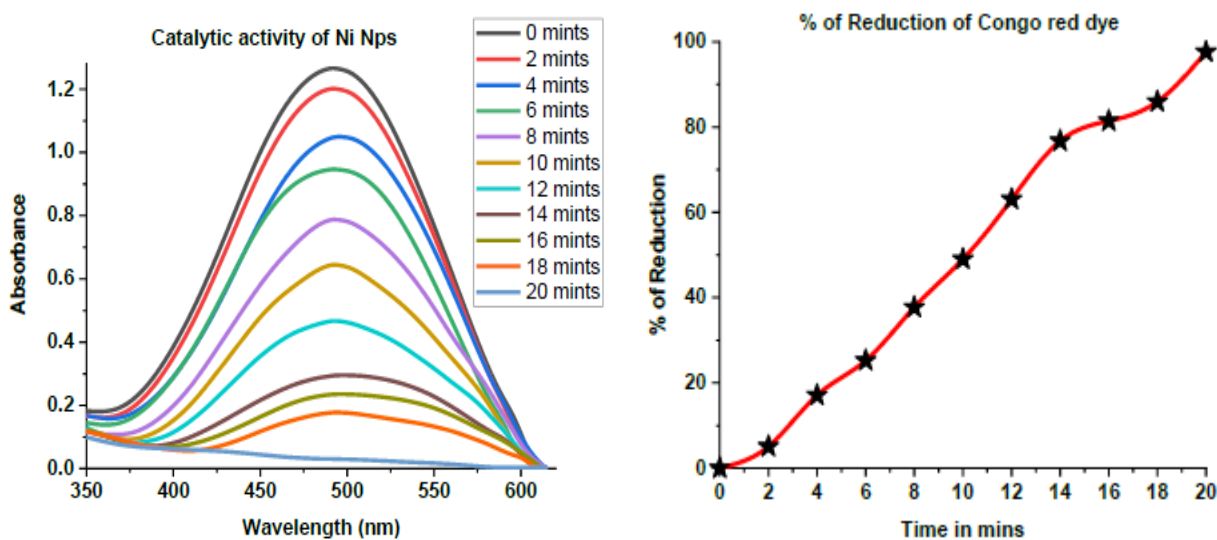


Fig. 7: a) Plot of catalytic activity of Ni NPs, b) % of reduction of CR by Ni NPs

#### 4. CONCLUSION

Ni nanoparticles were successfully manufactured utilising a simple and environmentally friendly method. The XRD study confirmed the FCC crystal structure with Fm-3m space group of Ni NPs. The TEM and SAED results were quite similar to the XRD data. According to the FTIR analysis, the polyphenols and alkaloids in the aqueous extract acted as reducing and capping agents, resulting in stable Ni NPs. Furthermore, Biogenic Ni NPs shown substantial antioxidant and catalytic activity against DPPH and Congo red (CR) dye. The outcomes of this study suggests to a feasible technique for producing NP by employing a green method for treating industrial effluents containing organic dyes produced by various industries.

#### Conflicts of interest

The authors, declares that there is no conflict of interest.

#### Source of Funding

The authors did not receive any found for this work

#### 5. REFERENCES

- Radoor S, Karayil J, Parameswaranpillai J, Siengchin S. *Sci Rep*, 2020; **10(1)**:15452-15466.
- Vital RK, Saibaba KVN, Shaik KB. *J Bioremediation Biodegrad*, 2016; **07**:371.
- Hernández-Zamora M, Martínez-Jerónimo F. *Environ Sci Pollut Res*, 2019; **26(12)**:11743-11755.
- Hernández-Zamora M, Perales-Vela HV, Flores-Ortiz CM, Cañizares-Villanueva RO. *Ecotoxicol Environ Saf*, 2014; **108**:72–77.
- Nayak A, Sahoo JK, Sahoo SK, Sahu D. *Int J Environ Anal Chem*, 2020; **10**:1-22.
- Debnath P, Mondal NK. *Environ Nanotechnology, Monit Manag*, 2020; **14(January)**:100320.
- Mahapatra A, Mishra BG, Hota G. *Ceram Int*, 2013; **39**:5443–5441.
- Ismail M, Khan MI, Khan SB, Khan MA, Akhtar K, Asiri AM. *J Mol Liq*, 2018; **260**:78–91.
- Taj MB, Alkahtani MDF, Raheel A, Shabbir S, Fatima R, Aroob S, et al. *Sci Rep*, 2021; **11(1)**:1–19.
- Mall ID, Srivastava VC, Agarwal NK, Mishra IM. *Chemosphere*, 2005; **61(4)**:492–501.
- Singh J, Kalamdhad AS, Koduru JR. *Nanotechnol Environ Eng*, 2017; **2(1)**:2-10.
- Jaji ND, Lee HL, Hussin MH, Akil HM, Zakaria MR, Othman MBH. *Nanotechnol Rev*, 2020; **9(1)**:1456–1480.
- Abramczyk H, Paradowska-Moszkowska K, Wiosna G. *J Chem Phys*, 2003; **118(9)**:4169–4175.
- van den Berge J, Vos J, Boelens R. *Int J Water Resour Dev*, 2022; **38(1)**:173–191.
- Unuofin JO, Oladipo AO, Msagati TAM, Lebelo SL, Meddows-Taylor S, More GK et al. *Arab J Chem*, 2020; **13(8)**:6639–6648.
- Zsembik BA. *Health issues in latino families and households. Handb Fam Heal Interdiscip Perspect*. 2006; **6(20)**:40–61.
- Asif M. *Chem Int*, 2015; **1(1)**:35–52.
- Gupta PC. *Int J Pharm Pharm Sci*, 2012; **4(SUPPL.3)**:62–68.
- Mohan Kumar K, Sinha M, Mandal BK, Ghosh AR, Siva Kumar K, Sreedhara Reddy P et al. *Spectrochim Acta - Part A Mol Biomol Spectrosc*, 2012; **91**:228–233.
- Barzinjy AA, Hamad SM, Aydın S, Ahmed MH, Hussain FHS. *J Mater Sci Mater Electron*, 2020; **31(14)**:11303–11316.
- Khan SA, Shahid S, Lee CS. *Biomolecules*, 2020; **10(6)**:458-462.
- Sudhasree S, Banu AS, Brindha P, Kurian GA. *Toxicol Environ Chem*, 2014; 1–12.
- Imran M, Ghulam A, Rani A, Aihetasham A, Mukhtar M. *Environ Nanotechnology, Monit Manag*, 2018; **9(December 2016)**:29–36.
- Din MI, Tariq M, Hussain Z, Khalid R. *Inorg Nano-Metal Chem*, 2020;1–6.
- Khalil MMH, Ismail EH, El-Baghdady KZ, Mohamed D. *Arab J Chem*, 2014; **7(6)**:1131–1139.
- Mohamad NAN, Jai J, Arham NA, Hadi A. In: *Proceedings - 2013 IEEE International Conference on Control System, Computing and Engineering, ICCSCE 2013*. 2013.
- Mohan Kumar K, Sinha M, Mandal BK, Ghosh AR, Siva Kumar K, Sreedhara Reddy P. *Spectrochim Acta - Part A Mol Biomol Spectrosc*, 2012; **91**:228–233.
- Heydari S, Aliakbarkhani ZS. *Int. J. Nanosci. Nanotechnol*, 2020; **16(3)**:153-165.
- Khalil MMH, Ismail EH, El-Baghdady KZ, Mohamed D. *Arab J Chem*, 2014; **7(6)**:1131–1139.
- Noukelag SK, Mohamed HEA, Moussa B, Razanamahandry LC, Ntwampe SKO, Arendse CJ, et al. *Mater Today Proc*, 2019; **36(XXXX)**:245–250.

31. Bhat SA, Zafar F, Mondal AH, Kareem A, Mirza AU, Khan S, et al. *J Iran Chem Soc*, 2020; **17(1)**:215–227.
32. Helan V, Prince JJ, Al-Dhabi NA, Arasu MV, Ayeshamariam A, Madhumitha G, et al. *Results Phys*, 2016; **6**:712–718.
33. Kalwar NH, Nafady A, Sirajuddin, Sherazi STH, Soomro RA, Hallam KR, et al. *Mater Express*, 2015; **5(2)**:121–128